CrystEngComm

Accepted Manuscript

ROYAL SOCIETY OF CHEMISTRY

www.rsc.org/crystengcomm

Controlling the Crystallisation of Oxide Materials by Solvothermal Chemistry: Tuning Composition, Substitution and Morphology of Functional Solids

Craig I. Hiley, and Richard I. Walton*

Department of Chemistry, University of Warwick, Coventry, CV4 7AL.
E-mail: r.i.walton@warwick.ac.uk

Abstract

We provide an overview of currently emerging areas in the solvothermal synthesis of polycrystalline oxide materials that illustrate how tailoring synthesis may be possible to target the formation of functional solids. We illustrate various levels of control in preparation of functional oxides with interesting structures and new chemistry by choosing examples of three aspects of recent chemistry: (1) materials discovery (2) substitutional chemistry and (3) adjustment of crystal morphology and size. This includes new oxides of ruthenium, iridium and of bismuth, novel substitutional chemistry of CeO_2 and TiO_2, and control of crystal form of binary and ternary oxides. The accumulated research illustrates the potential for fine control of the properties of materials by targeted crystallisation of solid oxides with selected chemical composition and particle shape and dimensions from the nanoscale to the micronscale. These benefits uniquely arise from chemical variation possible by use of solution-mediated crystallisation. We conclude by discussing how future work must focus on developing predictive synthesis, where synthesis conditions could be selected to design a solid material with desired properties.

1. Introduction

The study of the properties of oxides has a long history and this leads to functionalities that are well-established in numerous well-known applications, from everyday uses to state-of-the-art technologies.[1] Contemporary applications in the fields of energy, electronics, heterogeneous catalysis and magnetism drive ongoing research into new ways of preparing oxide materials in new forms.[2] This Highlight is focussed upon chemical routes to polycrystalline, powdered samples of oxides; this is the form that many are used directly (consider high surface area heterogeneous catalysts) or available for easily processing into

devices (such as densified ceramics or as layers and coatings). At the present time particular emphasis is placed on physical properties emergent with nanoscale structure in the solid state. Alongside crystal morphology control, substitutional chemistry, partial replacement of one metal by another whilst retaining average crystal structure, continues to play a key role in tuning properties of oxides, thus most functional oxides are ternary, or higher, systems.[3]

Conventional synthesis approaches to polycrystalline samples of mixed-metal oxides involve elevated temperatures.[4] Heating in air is easily carried out to induce reaction and crystallisation and, if necessary, provides a convenient way to oxidise appropriate precursors with often no need to control gas atmosphere, as might be the case for other classes of inorganic materials (nitrides, or sulfides, for example). In the simplest case, for the preparation of a ternary oxide $A_xB_yO_z$ a mixture of binary oxides xAO_n and yBO_m would be ground together and heated, typically to temperatures in excess of 1000 °C. Such solid-state reactions may require repeated cycles of heating and grinding to achieve homogeneity on the atomic scale, and while this may be aided by the use of carbonates that decompose *in situ* with release of CO_2 (*i.e.* calcination), the reactions are inherently inefficient since they rely on diffusion of ions in the solid state, which has a large energetic barrier to overcome. The use of precursor chemistry is well established, whereby an amorphous precipitate, which already includes the desired atomic mixing of elements, is first prepared and then heated to induce crystallisation, often at lower temperatures than the direct solid-state reactions. Such sol-gel or co-precipitation (generally *chimie douce*) procedures have been well documented,[5] but still rely on the use of high temperatures in the finally annealing step and thus preclude the isolation of metastable compositions or structures and some loss of control of crystal morphology is inevitable.

In this Highlight we will describe recent advances in direct crystallisation of oxide materials from solution using *solvothermal* conditions (or *hydrothermal* when water is used as the solvent). The discussion thus focuses around synthesis methods that use a solvent heated close to or above its boiling point in a sealed system to bring about solubilisation of otherwise insoluble reagents and crystallisation of desired materials from the resulting medium.[6] Our article is divided into three sections to illustrate levels of control emerging in preparation of materials with interesting structures and new chemistry: (1) materials discovery, (2) substitutional chemistry to control properties, and (3) adjustment of crystal morphology and size. Our overview of the literature is not intended to be exhaustive: there are already review articles about the historical development of solvothermal synthesis of

dense ceramic materials[7] and the use of hydrothermal methods for the growth of large crystals.[8] Furthermore, some recent review articles focus upon specific aspects of hydrothermal oxide chemistry, such as understanding crystallisation mechanisms,[9] as well as the benefits of solvothermal synthesis of particular classes of materials.[10-13] All of our chosen examples are all solvothermal *synthesis*: the material is crystallised as phase-pure powder from the solution without the need for any further annealing or calcination. As will be apparent, this allows the formation of unusual crystal morphologies, unique chemical compositions, or polymorphs of materials that would otherwise be inaccessible by any method that employs high temperature as a reaction parameter.

2. Materials Discovery: Crystallisation of New Structures and Compositions

In this first section we will include examples of how solvothermal chemistry can be used to isolate materials with either structures or compositions never before reported, and not (yet) accessible by other synthetic routes. This is field of materials discovery, and from the point of view of a chemist is perhaps the most appealing benefit in exploring new reaction conditions for the synthesis of solids. We will take two examples from our own work in the chemistry of precious metals to illustrate this idea, the cases of ruthenates and of iridates, and a third example from others' work in the field of superconducting perovskite oxides. Complex ruthenium and iridium oxides are of interest in heterogeneous catalysis,[14] and in the electrocatalytic splitting of water.[15] Recently their magnetic and electronic properties have been part of the current focus on properties of oxides of 4*d* and 5*d* elements due to strong correlated electronic behaviour and strong spin-orbit coupling, not seen in 3*d* analogues.[16] The range of striking magnetic and electronic properties of ruthenates[17] is exemplified by superconductivity in Sr_2RuO_4,[18] ferromagnetism in $SrRuO_3$,[19] and non-Fermi-liquid behaviour in $La_4Ru_6O_{19}$.[20] Similarly, iridates have attracted much interest for their complex physics properties, such as frustrated magnetism and topological insulating behaviour in iridate pyrochlores.[21] Around ten years ago Müller-Buschbaum systematically reviewed the structural chemistry of ruthenates[22] and iridates,[23] and those articles provide useful catalogues of materials known at the time, including examples prepared by a variety of synthesis methods.

As with all transition-metal containing materials the concept of oxidation state is an informative way of accounting for the number of valence electrons associated with the metal centres when rationalising properties such as magnetism or conductivity. From a synthetic

chemistry point of view, the synthesis of ruthenates present an interesting challenge since a wide range of oxidation states of Ru in oxides are accessible in ruthenium oxides, ranging from +2 (in $SrFe_{0.5}Ru_{0.5}O_2$, a material accessed by topochemical reduction of a parent phase[24]) through to +8 (in RuO_4), possibly the largest range of oxidation states seen for any element in its oxide chemistry. Mixed-valent materials are also possible.[17] Iridium shows a smaller range of oxidation states in bulk oxides of +3 to +6 (although it is interesting to note that recently the +9 oxidation state has recently been reported in the species $[IrO_4]^+$, detected spectroscopically[25]), and again synthetic conditions must be carefully chosen if control of metal oxidation state is to be achieved. When preparing new complex ruthenates and iridates, highly oxidising environments are often required to access oxidation states of the metals higher than +4, and, indeed, to prevent reduction to the metal itself, however high partial oxygen pressure at elevated temperatures can lead to formation and volatilisation of considerable quantities of $Ru^{VIII}O_4$ in the case of Ru, making control of composition challenging. This is where hydrothermal chemistry provides an interesting possibility in the control of oxidation states of Ru and Ir, particularly since oxidising or reducing conditions can be provided in solution with sacrificial reagents whose decomposition leads to soluble side products after reaction.

We initially considered the hydrothermal chemistry of iridium since the solution chemistry of the element is rather less explored than others. Taking inspiration from earlier hydrothermal synthesis of alkali-earth titanates under hydrothermal conditions,[11] we explored the reactivity of iridium chloride with alkali-earth salts in aqueous alkali solutions.[26] This lead to the crystallisation of a set of hydroxides (rather than oxides), Figure 1 (a-c), in which the oxidation state of iridium is +4, as confirmed by Ir L_{III}-edge XANES (X-ray absorption near edge structure) spectroscopy. These are all novel materials: $BaIr(OH)_6{\cdot}H_2O$ and $Sr_2Ir(OH)_8$ are new compositions isostructural with known Pt and Sn hydroxides, respectively, while $Ca_2IrF(OH)_6{\cdot}OH$ has a unique structure. In the last case the inclusion of fluoride resulted from the use as NaF as a mineraliser during synthesis. All were formed as large enough single crystals for crystallographic analysis. Hydroxides, however, are inherently unstable thermally and also reactive to even dilute acid conditions, which might limit their applications. Hence we adjusted the synthesis conditions to explore the possibility of isolating iridates; thus by adding peroxide (either as hydrogen peroxide or, more conveniently as solid Na_2O_2) under similar conditions (aqueous NaOH as the reaction medium, heated to 200 – 240 ° C) two novel oxides crystallised as polycrystalline powders. Their structures were refined from powder neutron diffraction data, Figure 1 (d-e). Ir L_{III}-

edge XANES spectroscopy allowed confirmation of the Ir oxidation state, which was between +4 and +5, higher than in the hydroxides, due to the oxidising hydrothermal synthesis conditions. $(Na_{0.27}Ca_{0.59})_2Ir_2O_6{\cdot}0.66H_2O$ is a new pyrochlore (see below for more discussion of pyrochlores) while $Na_{0.8}Sr_{2.2}Ir_3O_{10.1}$ is a novel $KSbO_3$-structured phase. Sodium is included in both structures, and this comes from the aqueous NaOH used as the reaction medium. While these phase possess dense structures, of the type expected to be produced by conventional solid-state synthesis methods, upon heating both materials collapse little above 400 ^oC, with phase separation to mixtures of other phases. This shows their metastable character and suggests that the materials would be inaccessible under conventional synthesis conditions.

In the case of ruthenates we developed a simpler strategy to providing oxidising conditions and used alkali-earth peroxides in combination with potassium perruthenate ($KRu^{VII}O_4$) in pure water (*i.e.* with no other mineraliser) and thus were able to produce a set of alkali-metal ruthenates (oxyhydroxides for the barium materials).[27-29] Figure 2 shows a phase-diagram representation of the compositions of the new materials, plotted along with all reported analogous compounds in the literature. All of the hydrothermally prepared materials contain Ru in (average) oxidation state +4.7 or higher, up to +5.5, as verified by bond valence sums from the refined crystal coordinates and Ru K-edge XANES spectroscopy. As with the iridates prepared hydrothermally, the ruthenates are all metastable and begin to phase separate upon heating in air at ~400 °C. The composition space occupied by the hydrothermally-prepared samples in Figure 2, appears to be distinct from the materials prepared using conventional synthesis methods. The solution chemistry used in synthesis more commonly allows access to higher oxidation states of ruthenium, compared to phases prepared by solid-state reactions, and also mixed-valent materials also appear more frequently. The new phases are metastable and all collapse on heating, phase separating into materials that contain Ru(IV); this illustrates how they would be difficult to isolate using conventional high temperature reactions. The phase $SrRu_2O_6$ has proved to be of particular interest since it shows unusually high temperature magnetic ordering, with antiferromagnetic order persisting to ~560 K.[29] This is unprecedented in a layered material and understanding this phenomenon has been the focus of attention by several independent research groups.[30] When barium is used as the partner metal two new oxyhydroxides are formed depending on the Ba:Ru molar ratio used in the synthesis: $Ba_2Ru_3O_9(OH)$ and $Ba_4Ru_3O_{10.2}(OH)_{1.8}$. The former has a novel structure with puckered layers of edge- and corner-sharing Ru(V) octahedra,[27] while the latter is an example of a previously unreported, complex hexagonal

perovskite with a unique 8H stacking sequence with partially occupied sites for Ru in average oxidation state +4.75.[28]

The use of $KRuO_4$ as an oxidising reagent has been subsequently used by Jansen and co-workers to prepare a novel mixed-metal Ru(V) oxide under hydrothermal conditions: by reaction with freshly precipitated Ag_2O in water at 190-200 °C a new polymorph of Ag_3RuO_4 crystallises directly.[31] The phase was formed as large enough single crystals for structure solution, which revealed a novel cation-ordered NiAs structure, with segregated $[Ru_4O_{16}]^{12-}$ units that behave as molecular magnetic clusters.

The $A_2B_2O_7$ pyrochlore structure has emerged as a common link between the hydrothermal chemistry of iridates and ruthenates (see Figures 1 and 2) and a number of new compositions in this family have now been reported. Figure 3 describes the pyrochlore structure with a compilation of the A-site metals that we[26, 32-34] and others[35] have included by hydrothermal synthesis in ruthenates and iridates (*i.e.* with B = Ru or Ir).

While the iridate pyrochlores have interesting magnetic properties,[21] and the magnetism of Ru(IV)-containing pyrochlores is also of fundamental interest,[36] we have additionally studied the properties of the ruthenate and iridate pyrochlore family as novel electrocatalyst materials.[33, 34] In particular their use in electrochemical oxygen evolution from water, of relevance for applications such as electrolysers and in polymer electrolyte membrane fuel cells, is topical. The range of composition ranges possible in the pyrochlore structure is particularly useful for heterogeneous catalysis applications for a number of reasons. Firstly, because the pyrochlore structure has a tendency for various types of oxide-ion disorder, with either displacement from its ideal site towards a fluorite-like structure, or partial replacement by water, hydroxide or monovalent anions, aided if the metal sublattice can adjust metal oxidation state;[37] this can give rise to redox properties in the solid state. Secondly, because variety of A and B site substitutions are possible involving many chemical elements and hence the properties can be fine-tuned by composition, allowing, for example, interatomic separation to be adjusted, or further control of oxidation states, to give, for example, conducting oxides. One major challenge in the field of electrocatalysis area of chemistry is to discover catalysts that are robust to acid conditions, where at low pH many oxide materials dissolve: oxides of iridium in particular are suited for this chemistry and addition of ruthenium enhances activity (albeit at the expense of stability).[38] We have recently shown how mixed ruthenate-iridate pyrochlores present a step forward in developing acid-resilient electrocatalysts for this application, and how the materials prepared by

hydrothermal synthesis provide nanocrystalline powders that can easily be fabricated into robust electrodes.[34] Although the use of precious-metals may be economically inhibitive the pyrochlores provide a way of diluting the use of Ru or Ir since the partner A site metal(s) are present in a similar molar quantity.

Another important example of materials discovery by hydrothermal chemistry is provided by the work of Kumada and co-workers who have prepared a family of superconducting bismuthate perovskites by direct hydrothermal crystallisation, Figure 4.[39-42] This was inspired by the long-known $BaBi_{1-x}Pb_xO_3$ and $Ba_{1-x}K_xBiO_3$ materials where K or Pb are introduced into $BaBiO_3$ to give mixed valent Bi^{3+}/Bi^{5+} resulting in superconductivity with transition temperatures up to ~30 K.[43] For the hydrothermally prepared materials of Kumada, the synthesis method employs the oxidising Bi(V) salt $NaBiO_3{\cdot}2H_2O$ as a reagent under basic conditions at 180 – 220 °C, with addition of other metal salts.

The first example, formulated as $(Ba_{0:75}K_{0:14}H_{0:11})BiO_3{\cdot}nH_2O$, is a mixed A-site material with Ba^{2+}, K^+ and H_2O. The A site substituents are ordered with distinct sites for Ba^{2+} and (K,H_2O), Figure 4b. This material shows a superconducting transition of ~8K, as measured by the onset of diamagnetism, yet is metastable: upon heating in air water is lost above 500 °C to give a Ba,K mixed perovskite.[39] The A-site-ordered $(Na_{0.25}K_{0.45})Ba_3Bi_4O_{12}$ has essentially the same $A'A''_3B_4O_{12}$ structure with the A' site randomly occupied by both Na and K along with vacancies, and the A'' site by Ba; the material shows a *T*c of ~27 K, and decomposes above 600 °C with loss of O_2 and reduction of Bi^{5+} to Bi^{3+}.[40] The mixed lead-bismuth B-site perovskite $(Ba_{0.82}K_{0.18})(Bi_{0.53}Pb_{0.47})O_3$ was crystallised from $PbBi_2O_{5.9}{\cdot}H_2O$ (itself prepared from $NaBiO_3{\cdot}nH_2O$ in $Pb(NO_3)$ at room temperature) and $Ba(OH)_2$ in aqueous KOH at 240 °C. This 'double double' perovskite has mixed A-site and mixed B-site, with randomly distributed Ba,K and Bi,Pb, respectively, Figure 4a. This compound exhibits a superconducting onset of ~ 22.8 K, and its thermal decomposition occurs above 600 °C.[41] Finally, $KBa_3(Bi_{0.89}Na_{0.11})_4O_{12}$ is a mixed B-site material $A'A''_3B_4O_{12}$ with a large shielding volume fraction, exceeding 100%, and onset of superconductivity at ~ 31.5 K.[42] This set of materials illustrates well the idea of materials discovery: where novel compositions representing new superconducting phases are found in a family first studied more than 40 years ago.

3. Control of Oxide Properties by Substitutional Chemistry

Although mentioned above for the case of pyrochlores and perovskites, in this section we discuss how substitutional chemistry can be used to modify properties of oxides. We will emphasise how the hydrothermal method allows inclusion of unusual elements in binary systems to then modify the properties of the parent material for specific applications. First we consider the case of cerium dioxide (ceria). This material has been extensively studied for its important applications in heterogeneous catalysis, where it provides a redox-active support in which the ready interconversion between Ce^{4+} and Ce^{3+} allows release and uptake of oxygen.[44] When loaded with small particles of precious metal the resulting cooperative effect finds use in areas such as water-gas shift catalysis, the conversion of CO and water to hydrogen and CO_2, which is of relevance for purifying hydrogen produced from steam reforming,[45] and in automotive three-way catalysts, which are under continual development to meet ever stringent legislative demands.[46]Also emerging are other catalysis applications for precious-metals supported on ceria in oxidation catalysis, such as in the methane oxidation reaction.[47] and in solar induced water splitting.[48] The properties of ceria have also been explored in other areas, such as abrasive agents for chemical mechanical planarisation of integrated circuits,[49] cosmetic UV-shielding,[50] and humidity sensing.[51]

Substitution of Ce^{4+} in the fluorite structure of CeO_2 by other cations is a widely used strategy for tuning the redox properties of the solid. Replacement by an aliovalent cation, such as a trivalent rare-earth (La^{3+}, Gd^{3+}, for example), introduces oxide-ion defects that may enhance oxide-ion mobility and redox properties, while addition of an isovalent cation of different size can give local structural distortion and lattice strain, also enhancing properties associated with oxide-ion mobility, and the case of Zr^{4+} has been well documented.[52] Figure 5 presents a survey of all the chemical elements that have been included in ceria, using a variety of synthesis methods, but use of solvothermal synthesis is highlighted, where it can be seen that these routes often permit the highest level of elemental substitution.[53] This has often been proved experimentally by a combination of lattice parameter expansion (or contraction) and local structural probes such as Raman spectroscopy. We choose some selected examples to show the benefit of solvothermal synthesis in this chemistry.

In early work in this field Li *et al.* showed how Fe could be included into nanocrystalline ceria by hydrothermal crystallisation from aqueous solutions of $Ce(NO_3)_3$ and $Fe(NO_3)_3$ in the presence of NaOH, despite the fact that mixed oxides of Ce and Fe cannot be

accessed by high temperature solid-state chemistry.[54] Materials of composition $Ce_{1-x}Fe_xO_2$ with x up to 0.2 could be produced, with a lattice contraction and EPR spectroscopy proving the presence of octahedral Fe^{3+}. The authors proposed that Fe^{3+} must be present in interstitial sites, and yet with a low level of oxide-ion deficiency. However, the issue of incompatibility of octahedral substituents into the ceria structure that contains cubic (eight-coordinate) metal sites is one that has not yet been resolved, and it is clear that detailed structural studies are needed to understand properly how such a dopant can be included in the ceria structure. The incorporation of other trivalent cations into ceria can result in considerable distortion of the average structure. In the case of Bi^{3+} this is because of the unsymmetrical coordination preference of this 'lone-pair cation', although it may be noted that Bi_2O_3 does have an (average) oxide-deficient fluorite structure at high temperature.[55] In our hydrothermal synthesis we found that using $NaBiO_3{\cdot}2H_2O$ as an oxidising source of Bi, in combination with $CeCl_3$ in aqueous NaOH at 240 °C gave nanocrystalline $Ce_{1-x}Bi_xO_{2-\delta}$ with x up 0.6.[56] In this case the presence of oxide-ion deficiency is expected since XANES spectroscopy proved that Bi is present in the +3 oxidation state, and pair distribution studies derived from neutron scattering showed how the local structure is distorted to accommodate the bulky substituent but with the Bi residing close to the expected Ce sites in the structure. Bi-substituted ceria undergoes structural collapse under strongly reducing conditions, with extrusion of metallic bismuth upon heating in even dilute hydrogen: this illustrates the instability of such a distorted and heavily substituted ceria,[56] although the material may still be beneficial for other catalytic applications that involve oxidative conditions.[57]

While the use of precious metal nanoparticles supported on ceria is commonplace, where an atomic scale interaction between the precious metal and the ceria surface gives catalysis properties,[44] it is interesting to consider the possibility of including a precious-metal cation within the ceria lattice. This is something difficult to do by high temperature annealing due to the high likelihood of reduction of any precious metal salt or oxide into the metallic state, hence solution synthesis offers a viable proposition. We have thus shown recently how Pd may be included within the ceria lattice, formally substituting Ce^{4+} by Pd^{2+} to give compositions $Ce_{1-x}Pd_xO_{2-\delta}$, where $0 \leq x \leq 0.15$.[58] This was achieved by a hydrothermal reaction involving $CeCl_3{\cdot}7H_2O$ and $PdCl_2$ in aqueous NaOH with oxidising conditions provided by the use of hydrogen peroxide. This gave nanocrystalline powders with a homogeneous distribution of Pd, for which EXAFS spectroscopy was used to prove the presence of square-planar Pd^{2+} in interstitial positions in the fluorite structure, Figure 6.

Despite shorter Pd-O distances compared to Ce-O, the lattice is expanded when Pd is added: this is because of its location in the otherwise unoccupied square of oxide ions forces expansion to accommodate the coordination preference of Pd^{2+}.

Another binary oxide at the focus of attention for its widespread applications is TiO_2: research centres upon properties for use in photocatalysis, such as in solar energy conversion devices, destruction of organic pollutants or in water splitting as a route to hydrogen and oxygen.[59] TiO_2 differs from the case of CeO_2 in that it exists as a number of polymorphs, all stable at close to room temperature and all containing octahedral metal centres: anatase and rutile are the two most common forms, with latter being the thermodynamically most stable and hence the phase that results upon any prolonged annealing. Solvothermal synthesis conditions have already been proven to allow selective formation of one TiO_2 polymorph over another often in nanostructured form,[60] and in recent work desirable mixtures of anatase and rutile polymorphs have been produced by hydrothermal treatment to convert amorphous interfacial material into crystalline solid.[61] An additional focus is, however, the inclusion of other cations to adjust its light absorption properties and hence to optimise photocatalysis. Solvothermal synthesis plays a role here and the past few years there have been reports of inclusion of a range of chemical elements into TiO_2. Some of these may be anticipated since other tetravalent metals adopt the rutile structures, as found for SnO_2 or RuO_2, and indeed these can be substituted in rutile TiO_2 to give solid-solutions across the whole composition range from hydrothermal reactions such as $Ti_{1-x}Sn_xO_2$,[62] or with controlled levels of Sn inclusion to optimise photoelectrochemical properties;[63] alternatively very small amounts of substitution may be beneficial such as in the case of $Ti_{1-x}Ru_xO_2$ where addition of even a small amount of Ru, 0.8 mol %, gives enhanced visible-light-driven H_2 production over pure TiO_2.[64] For other substituents, the anatase structure is produced by solvothermal crystallisation. For example, La^{3+} can be included in TiO_2 by a solvothermal reaction from titanium butoxide and $La(NO_3)_3$ in an acetic acid-hydrofluoric acid mixture, and Zhang *et al.* produced nanoscale plates of the La-TiO_2 anatase directly onto an transparent conductive fluorine-doped tin dioxide substrate.[65] Although annealing was needed to form highly crystalline materials, this illustrates the scope of the method for forming devices based on layers of solvothermally deposited complex-oxide films; in this case photocatalytic degradation of model organics was studied. By crystallisation from ethanolic solutions of titanium(IV) isopropoxide and cerium nitrate hexahydrate, Ce-substituted TiO_2 can be formed in the anatase structure: in this case the Ce is predominantly present as Ce(III), something difficult to achieve by any method that involves post-synthesis annealing due to its

ready oxidation to Ce(IV), but in this as-made form at low levels, the material shows photocatalytic hydrogen production from water under UV irradiation.[66]

As well as cation substitution, anion substitution is another approach for modifying the electronic properties of oxides and for TiO_2 a number of solvothermal approaches have developed to achieve this. While replacement of oxide by other monatomic anions such as nitride or fluoride in solvothermal reactions has been reported,[67] Liu *et al.* considered the case of carbonate inclusion and produced substituted anatase TiO_2 microspheres by a solvothermal reaction between titanium alkoxide and acetone at 200 °C, where an aldol condensation is the driving force for reaction.[68] Computational modelling allowed the location of carbonate in the lattice to be proposed, Figure 7, and also provided a rationale for the narrow band gap of the substituted material compared to pure anatase; this was proven by successful hydrogen evolution in photo-catalytic water splitting with visible light. It would be difficult to envisage carbonate substitution by any other method since high temperatures would inevitably lead to thermal decomposition.

4. Solution Chemistry to Control Crystal Morphology and Form

The examples we have so far chosen in our review illustrate how solution chemistry can be used to control the composition and/or crystal structure of new oxide materials, whether in stoichiometric systems, or in cases where substitutional chemistry is performed. A further important aspect in the tuning of properties of any real material for practical applications is the ability to engineer the size and shape of individual crystals making up a polycrystalline powder. The morphology of a crystal is what defines its applications, beyond the underlying inherent properties of the chemical structures, since materials must be processed, shaped, and formed into devices, and, in addition, the surface chemistry of crystals can dictate the reactivity of the material, in catalysis, for example. Thus solution-based synthesis is an extremely attractive proposition for control of crystallite size and shape, since crystal growth occurs under moderate conditions without the need for high temperature annealing that might destroy any intricate crystalline morphologies. Further, there are many experimental variables that potentially allow crystal growth to be fine-tuned: solution concentration, temperature, heating (and cooling) rates, pH, and inclusion of solution additives that might stabilise certain crystal faces, *etc.* Wu *et al.* have recently reviewed some of the fundamentals of shape control

of solids from solution crystal growth.[13] In this section we will take some recent examples of oxide chemistry from the literature, from a variety of different researchers; these provide some striking examples of how solution chemistry is being used to produce unusual crystal morphologies of oxides under solvothermal conditions. As with the earlier sections, this is not a complete review of the literature: we instead have taken relevant examples that illustrate some key emerging trends that may in the future lead to routes to materials applicable in applications.

First we consider some binary oxides. Chen and Xue studied the crystallisation of Cu_2O using a hydrothermal method from Cu(II) nitrate in the presence of starch as reductant and various concentrations of NaOH at 120 °C.[69] They proved a remarkable dependence of crystallite size and morphology on simply the pH of the solution used, with evolution of shape from nanowires, through aggregated spheres and octahedra to truncated octahedra and cuboctahedra, Figure 8. A mechanism of formation was proposed in which the role of solution species, dictated by the pH dependence of redox potential of Cu^{2+}, was key to the resultant crystal form. Cu_2O has been the focus of much systematic study in this respect, with various reducing agents surveyed along with pH and reaction temperature giving intricate crystal forms that provide a useful model system for understanding hydrothermal crystal growth of oxide, and Chen *et al.* have reviewed this chemistry, along with analogous routes to other binary oxides such as CuO and MnO_2, with emphasis on their relevance for application in electrode materials for energy applications.[70]

Xu *et al.* studied the formation of the mixed-valent iron oxide spinel magnetite (Fe_3O_4) using a solvent mixture of ethylene glycol and H_2O with urea as an additive.[71] They showed an evolution of 50-facet Fe_3O_4 polyhedral crystals, Figure 9, by adjusting the reaction temperature, the reaction time, the amount of urea, the choice of iron precursor, and the volume ratio of ethylene glycol to water in the solvent mixture. The authors proposed that coordination of ethylene glycol to the iron at the crystal surface led to the high index {311} and {110} facets on the polyhedral nanocrystals.

Zinc oxide is a material that is focus of much attention for its applications arising from its semiconductivity and the control of crystal form may be of relevance for practical uses such as in sensors, field-effect transistors, optoelectronics and photocatalysis. Yin *et al.* used a mixed water-ethanol solvent system in the presence of glycine at 200 °C to form polycrystalline ZnO materials from zinc acetate dihydrate.[72] With increasing amount of water

in the solvent mixture the crystal shape was modified from assemblies of nanoparticles and discs, through pure discs to pure rod-shaped, Figure 10. While the mechanism of action of glycine was not established it clearly behaves as a potent growth modifier and the authors suggested that the change in solvent composition changed its solubility and hence mode of action.

Das *et al.* used citrate as a crystal growth modifier for ZnO under hydrothermal conditions and proposed that surface binding of the citrate directed the formation of hexagonal faces of the ZnO crystallites by match of the Zn---Zn interatomic distances with a favourable bonding mode of the polydentate ligand.[73] In this case, depending on citrate:Zn ratio, a variety of intricate crystal forms could be isolated. In a related study, Wang *et al.* used ethanolamine as a crystal habit modifier and produced ZnO with a variety of particle morphologies based upon primary needle-shaped crystallites.[74] It may be noted that earlier work has shown how much milder conditions can be used for the solution formation and crystal habit modification of ZnO: for example, Raula *et al.* used ascorbate as an additive and between 30 and 60 °C formed various shapes of hierarchical ZnO nanostructures from a range of different zinc salts with water as the main solvent.[75] This illustrates that strictly solvothermal conditions may not always be necessary, although it may be the case that upon heating at or above the boiling point the solubilisation of a much greater choice of reagents and additives may be possible.

The control of crystal form of ternary oxides also has proved possible by solvothermal synthesis. One prototypical material that has been studied in this respect is the perovskite $BaTiO_3$, well known for its dielectric properties in its tetragonal polymorph. Earlier work had proved that when using TiO_2 or alkali-metal titanates as starting materials under hydrothermal conditions then the size and shape of the $BaTiO_3$ formed was a direct replica of the size and shape of the titania or titanate precursor.[11] This retention of crystal form strongly suggests that little dissolution of the solid precursor takes place: either crystallisation occurs by transport of a second metal ion into the solid reagent or local dissolution occurs such that the reagent particles have a templating influence on the solid product that is formed. Some recent work by various groups has taken this 'shape preserving' synthesis route further to form intricate morphologies, with properties being measured to prove their potential use in applications.

Lamberti *et al.* produced vertically oriented TiO_2 arrays of nanotubes by ultra-fast anodic oxidation of titanium foils and then converted them to tubular structures of $BaTiO_3$ in alkali solutions of barium acetate at 150 – 200 °C.[76] At the lower temperatures, Figure 11, the

$BaTiO_3$ was partially in the paraelectric cubic phase, but for samples prepared at 200 °C for 24 hours, which retain the tubular morphology, electrical characterisation confirmed ferroelectric behaviour expected for the tetragonal phase. The coercive fields related to the tetragonal domain switching are higher than in bulk samples, which is characteristic of nanoconfinement of ferroelectric domains.

Caruntu *et al.* produced nanocrystalline $BaTiO_3$ from solvothermal reactions using various alcohols as solvents in the presence of NaOH and oleic acid with $Ba(NO_3)_2$ and $Ti(OBu)_4$ as precursors.[77] Size-control of the cubic crystals was demonstrated, depending on the concentrations of reagents used and the polarity of the solvent, Figure 12. The as-made particles are coated with oleic acid molecules on their surfaces and so are hydrophobic, allowing the formation of highly stable colloidal solutions in nonpolar solvents. The authors showed that upon oxidative cleavage of the oleic acid the surface molecules are converted into azelaic acid, thus adjusting the perovskite nanocrystals to be hydrophilic and dispersible in polar solvents. The significance of this post-synthesis modification and control of surface chemistry, is that this paves the way for controlled assembly of functional particles for the formation of, for example, hierarchical or composite structures. The same synthesis method was used for the related perovskites $BaZrO_3$, $PbTiO_3$ and $SrTiO_3$.[77]

Friderichs *et al.* also used oleic acid as a surface modifier, in this case to prepare monodisperse $SrTi_{1-x}Zr_xO_3$ nanocubes, of size ~10 nm, using a two-phase oil/water solvent mixture.[78] Their work has some significant novelty since they used an optically transparent autoclave from which the evolution of reaction at the oil/water interface could be followed. They also proposed a model for the evolution of crystal morphology, based on the steric constraints of the oleate moieties at the growing crystal surface.

Hydrothermal synthesis of perovskite manganites have attracted much attention since earlier work that proved that mixed-valent $AA'MnO_3$ with A = divalent alkali earth and A = trivalent rare-earth could be isolated by judicious choice of manganese precursors.[79] These materials are of interest for their magnetic and electronic properties, such as the presence of magnetoresistance. Furthermore, hexagonal polymorphs of the perovskite structure can be obtained for manganites, such as in the base of $BaMnO_3$, where hydrothermal routes form the 2H polytype,[80] and for $YMnO_3$ hydrothermal synthesis yields a layered hexagonal polymorph.[81] Recent work on the hydrothermal formation of manganites has focused on understanding crystal growth mechanism, and in the control of crystal form to produce novel nanostructures that might have unusual magnetic properties. González-Jiménez *et al.* made a

systematic study of the formation of 4H-$SrMnO_3$ under hydrothermal conditions using salts of Sr^{2+}, Mn^{2+}, and $[MnO_4]^-$ salts and aqueous KOH.[82] This work represents one of the most detailed investigations of the hydrothermal formation of a mixed-oxide, with extensive screening of sets of reaction conditions and in-depth analysis of the isolated products using advanced characterisation. This allowed the optimum conditions for the production of phase-pure perovskite to be established and various side products were identified: crucially by this hydrothermal method it was concluded that nanocrystalline 4H-$SrMnO_3$ could never be formed even at extremes of the pH range. The synthesis is also complicated by the formation of $K_{0.04}Sr_{0.16}MnO_2 \cdot nH_2O$ is formed as an intermediate, and other crystalline byproducts; nevertheless the 4H-$SrMnO_3$ that is formed is well ordered, with no evidence of extended defects. This work illustrates the complexity of hydrothermal oxide chemistry and the need to explore systematically synthesis conditions.

More complex manganites also have been prepared in unusual morphologies. Makovec *et al.* crystallised single-crystalline dendrites of the quaternary system $La_{1-x}Sr_xMnO_3$ using a hydrothermal method from metal salts of Sr^{2+}, La^{3+}, and Mn^{2+} in NaOH solution, without the use of any other solution modifiers.[83] In related work, Huang *et al.* found that use of ammonium salts allowed shape modulation of $La_{1-x}Sr_xMnO_3$; in this case solutions of $La(NO_3)_3$, $Sr(NO_3)_2$, $MnCl_2$ and $KMnO_4$ were used with the amount of Mn^{VII} and Mn^{II} in the precursors adjusted to give the desired average oxidation state of the product.[84] They showed a complex evolution of crystal morphology from cubic to multi-facetted, pyramidal clusters, Figure 13. The same group have also published an informative review article proposing how crystal facet tailoring in perovskite oxides may be possible by hydrothermal chemistry.[12] This concept can confer useful properties: for example in the case of $PbTiO_3$, Yin *et al.* found that $PbTiO_3$ nanocrystals with well-defined {111} facets from a hydrothermal method by using $LiNO_3$ as solution modifier, have enhanced visible-light photocatalytic activity for the photocatalytic degradation of the model organic methylene blue.[85]

5. Summary and Outlook

We have presented selected examples of the key papers from the recent literature that illustrate various advantageous aspects in the solvothermal crystallisation of oxide materials. This includes the discovery of new materials, both with unprecedented crystal structures or compositions, the inclusion of unexpected substituent elements in familiar structures, the

formation of intricate nano-scale or micro-scale structures. The use of oxidants in solution allows access to high oxidation states of second and third-two elements such as Ru and Ir: a convenient feature of this solution chemistry is the use of solid peroxides as reagents, which yield soluble decomposition products that can be washed away from the solid product. On the other hand, solution additives (organic carboxylic acids, amino acids, or simple inorganic ions) have been employed to modify crystal morphology, but even variation of pH can have similar effects. Shape-preservation of morphology is also proving a valuable strategy for controlling crystal form, where an oxide product has microstructure that mimics the form (size and shape of crystals) of a chosen precursor.

If solvothermal synthesis of oxides is truly to be controlled to give materials with properties tailored for application, clearly some predictive ability in synthesis is needed. At present while there hints of being able to achieve this, the wide variety of reaction parameters means that conditions used for the synthesis of one material are not necessarily transferable to another. The case of crystal habit modifiers clearly falls into this category, although some systematic trends are emerging in specific families of materials; for example solvothermal engineering of crystal facets in perovskite oxides.[12] It is clear that a detailed knowledge of crystallisation kinetics and mechanism is urgently required to put the solvothermal synthesis of oxide materials on a firmer fundamental basis. There have been huge advances in the use of *in situ* experimental probes to follow crystallisations within sealed reaction vessels, using for example, high energy X-rays at synchrotrons where structural information can be refined as a material evolves.[86]A particularly noteworthy development in this respect is the introduction of *in situ*, time-resolved pair distribution function analysis, where the evolution of short-range and long-range structure can be tracked by use of high energy X-rays (and hence large *Q*-range scattering data): this has allowed the emergence of binary oxides of cerium,[87] tin,[88] and tungsten[89] from hydrothermal reactions to be observed and pre-crystallisation building units to be proposed. High intensity synchrotron X-rays also allow other *in situ* experiments to be designed: for example, the use of small-angle X-ray scattering permits observation of large-scale structure such as particle size and porosity. Xia *et al.* used this to great effect to study the solvothermal formation of mesoporous TiO_2 (anatase) beads, with the evolution of porosity tracked in real time from solution at temperatures between 140 and 180 °C.[90] Together, these *in situ* studies provide the first information towards proposing crystallisation mechanisms to aid prediction of future syntheses. With greater access to facilities for such experiments available to many researchers, this should create a substantial

body of data to allow the effect of synthetic variables to be mapped and crystallisation to be understood.

Computer modelling is highly likely to play a part in understanding crystallisation and in predicting the formation of new materials. At the present time, however, while computer modelling is been significantly advanced to allow prediction of likely candidate structures for new materials,[91] there remains a huge disconnect with prediction of the synthetic chemistry needed to access them. Some recent works some promise in this area, however: for example, Raccuglia *et al.* recently described a machine-learning approach to predictive materials synthesis where by input of a database of failed, as well as successful, synthesis conditions, predictions of new reaction parameters could be made with a statistically significant success rate.[92] Notably this work was applied for the solvothermal crystallisation of organic-inorganic hybrid materials, so could conceivably be applied for the type of chemistry we have described in this Highlight. Earlier work, more than 20 years ago, by Lencka and Riman and co-workers applied thermodynamic calculations, using tabulated standard-state properties and solution activity coefficients, to allow stability-yield diagrams to be calculated showing pH regions for the successful hydrothermal crystallisation of ternary titanates, such as $BaTiO_3$ and $PbTiO_3$.[93] It would be interesting, and timely, to return to such calculations with the new examples described in this Highlight, where redox chemistry is an additional consideration and the greater synthetic complexity would benefit from a guided synthesis approach.

Another consideration when discussing materials synthesis is whether the production of materials for applications can be scaled up to produce the amounts needed for commercial use. In this respect it is interesting to note that there have been advances in the development of continuous flow technology that permit hydrothermal and solvothermal reactions to be performed to yield materials at a scale and in time viable for commercial manufacture.[94] This work includes a number of oxides spanning binary materials (CeO_2, TiO_2, Co_3O_4 *etc.*) to more complex systems ($Y_5Al_3O_{12}$, $KNbO_3$, $Ba_{1-x}Sr_xTiO_3$ *etc.*), and these can be formed as nanocrystalline powders with production rates of 100s of grams per hour or higher.[94] This points towards solvothermal oxide crystallisation being commercially viable in the future, as well as continuing to uncover new materials with interesting properties.

Acknowledgements

We thank Johnson Matthey plc and the EPSRC for the provision of an Industrial CASE Studentship for C.I.H. and colleagues at the Johnson Matthey Technology Centre, Sonning Common for their collaboration in our work on materials synthesis.

References

[1] P. A. Cox, *Transition Metal Oxides: An Introduction to Their Electronic Structure and Properties*, Oxford University Press, Oxford 1992; C. N. R. Rao and B. Raveau, *Transition Metal Oxides: Structure, Properties, and Synthesis of Ceramic Oxides*, 2nd edn., Wiley–VCH, New York and Weinheim, 1998; S. B. Ogale, T. V. Venkatesan and M. G. Blamire, eds., *Functional Metal Oxides: New Science and Novel Applications*, Wiley-VCH Verlag Weinheim, 2013

[2] E. W. McFarland and H. Metiu, *Chem. Rev.*, 2013, **113**, 4391-4427.

[3] Y. B. Mao, T. J. Park and S. S. Wong, *Chem. Commun.*, 2005, 5721-5735.

[4] P. Cousin and R. A. Ross, *Mater. Sci. Eng. A-Struct. Mater. Prop. Microstruct. Process.*, 1990, **130**, 119-125.

[5] C. J. Brinker and G. W. Scherer, *Sol-Gel Science: The Physics and Chemistry of Sol-Gel Processing* Academic Press Limited London 1990; J. Rouxel and M. Tournoux, *Solid State Ionics*, 1996, **84**, 141-149; J.-P. Jolivet, *Metal Oxide Chemistry and Synthesis: From Solution to Solid State*, Wiley VCH, Weinheim, 2000.

[6] K. Byrappa and M. Yoshimura, *Handbook of Hydrothermal Technology*, 2nd edn., Elsevier, Amsterdam, 2013

[7] A. Rabenau, *Angew. Chem., Int. Ed.*, 1985, **24**, 1026-1040; G. Demazeau, *J. Mater. Chem.*, 1999, **9**, 15-18; S. Somiya and R. Roy, *Bull. Mater. Sci.*, 2000, **23**, 453-460; S. H. Feng and R. R. Xu, *Accounts Chem. Res.*, 2001, **34**, 239-247; R. E. Riman, W. L. Suchanek and M. M. Lencka, *Ann. Chim. - Sci. Mater.*, 2002, **27**, 15-36; G. Demazeau and A. Largeteau, *Z. Anorg. Allg. Chem.*, 2015, **641**, 159-163.

[8] R. A. Laudise, *Chem. Eng. News*, 1987, **65**, 30-43.

[9] Y. Zhou, Y. H. Lin and G. R. Patzke, *Prog. Chem.*, 2012, **24**, 1583-1591.

[10] M. Niederberger, G. Garnweitner, J. Ba, J. Polleux and N. Pinna, *Int. J. Nanotech.*, 2007, **4**, 263-281.

[11] D. R. Modeshia and R. I. Walton, *Chem. Soc. Rev.*, 2010, **39**, 4303-4325.

[12] K. K. Huang, L. Yuan and S. H. Feng, *Inorg. Chem. Front.*, 2015, **2**, 965-981.

[13] Z. Wu, S. Yang and W. Wu, *Nanoscale*, 2016, **8**, 1237-1259.

[14] A. T. Ashcroft, A. K. Cheetham, J. S. Foord, M. L. H. Green, C. P. Grey, A. J. Murrell and P. D. F. Vernon, *Nature*, 1990, **344**, 319-321; J. A. Kurzman, L. M. Misch and R. Seshadri, *Dalton Trans.*, 2013, **42**, 14653-14667.

[15] N. F. Atta, A. Galal and S. M. Ali, *Int. J. Electrochem. Sci.*, 2012, **7**, 725-746.

[16] W. Witczak-Krempa, G. Chen, Y. B. Kim and L. Balents, *Ann. Rev. Condens. Matt. Phys.*, 2014, **5**, 57-82.

[17] R. J. Cava, *Dalton Trans.*, 2004, 2979-2987.

[18] K. Ishida, H. Mukuda, Y. Kitaoka, K. Asayama, Z. Q. Mao, Y. Mori and Y. Maeno, *Nature*, 1998, **396**, 658-660.

[19] R. J. Bouchard and J. L. Gillson, *Mater. Res, Bull.*, 1972, **7**, 873-&.

[20] P. Khalifah, K. D. Nelson, R. Jin, Z. Q. Mao, Y. Liu, Q. Huang, X. P. A. Gao, A. P. Ramirez and R. J. Cava, *Nature*, 2001, **411**, 669-671.

[21] B. J. Yang and Y. B. Kim, *Phys. Rev. B.*, 2010, **82**, 11.

[22] H. Müller-Buschbaum, *Z. Anorg. Allg. Chem.*, 2006, **632**, 1625-1659.
[23] H. Müller-Buschbaum, *Z. Anorg. Allg. Chem.*, 2005, **631**, 1005-1028.
[24] F. D. Romero, S. J. Burr, J. E. McGrady, D. Gianolio, G. Cibin and M. A. Hayward, *J. Amer. Chem. Soc.*, 2013, **135**, 1838-1844.
[25] G. Wang, M. Zhou, J. T. Goettel, G. J. Schrobilgen, J. Su, J. Li, T. Schloeder and S. Riedel, *Nature*, 2014, **514**, 475-477.
[26] K. Sardar, J. Fisher, D. Thompsett, M. R. Lees, G. J. Clarkson, J. Sloan, R. J. Kashtiban and R. I. Walton, *Chem. Sci.*, 2011, **2**, 1573-1578.
[27] C. I. Hiley, M. R. Lees, J. M. Fisher, D. Thompsett, S. Agrestini, R. I. Smith and R. I. Walton, *Angew. Chem., Int. Ed.*, 2014, **53**, 4423-4427.
[28] C. I. Hiley, M. R. Lees, D. L. Hammond, R. J. Kashtiban, J. Sloan, R. I. Smith and R. I. Walton, *Chem. Commun.*, 2016, **52**, 6375-6378.
[29] C. I. Hiley, D. O. Scanlon, A. A. Sokol, S. M. Woodley, A. M. Ganose, S. Sangiao, J. M. De Teresa, P. Manuel, D. D. Khalyavin, M. Walker, M. R. Lees and R. I. Walton, *Phys. Rev. B.*, 2015, **92**.
[30] D. J. Singh, *Phys. Rev. B.*, 2015, **91**, 214420; S. Streltsov, I. I. Mazin and K. Foyevtsova, *Phys. Rev. B.*, 2015, **92**, 134408; W. Tian, C. Svoboda, M. Ochi, M. Matsuda, H. B. Cao, J. G. Cheng, B. C. Sales, D. G. Mandrus, R. Arita, N. Trivedi and J. Q. Yan, *Phys. Rev. B.*, 2015, **92**, 100404; D. Wang, W.-S. Wang and Q.-H. Wang, *Phys. Rev. B.*, 2015, **92**, 075112; M. Ochi, R. Arita, N. Trivedi and S. Okamoto, *Phys. Rev. B.*, 2016, **93**, 195149
[31] B. E. Prasad, P. Kazin, A. C. Komarek, C. Felser and M. Jansen, *Angew. Chem., Int. Ed.*, 2016, **55**, 4467-4471.
[32] R. J. Darton, S. S. Turner, J. Sloan, M. R. Lees and R. I. Walton, *Crys. Growth Des.*, 2010, **10**, 3819-3823.
[33] K. Sardar, S. C. Ball, J. D. B. Sharman, D. Thompsett, J. M. Fisher, R. A. P. Smith, P. K. Biswas, M. R. Lees, R. J. Kashtiban, J. Sloan and R. I. Walton, *Chem. Mater.*, 2012, **24**, 4192-4200.
[34] K. Sardar, E. Petrucco, C. I. Hiley, J. D. B. Sharman, P. P. Wells, A. E. Russell, R. J. Kashtiban, J. Sloan and R. I. Walton, *Angew. Chem., Int. Ed.*, 2014, **53**, 10960-10964.
[35] L. R. Yao, D. Wang, W. Peng, W. W. Hu, H. M. Yuan and S. H. Feng, *Sci. China Chem.*, 2011, **54**, 941-946.
[36] R. Mani, M. Fischer, J. E. Joy, J. Gopalakrishnan and M. Jansen, *Solid State Sciences*, 2009, **11**, 189-194.
[37] M. A. Subramanian, G. Aravamudan and G. V. S. Rao, *Prog. Solid State Chem.*, 1983, **15**, 55-143.
[38] M. E. G. Lyons and S. Floquet, *Phys. Chem., Chem. Phys.*, 2011, **13**, 5314-5335.
[39] H. Jiang, N. Kumada, Y. Yonesaki, T. Takei, N. Kinomura, M. Yashima, M. Azuma, K. Oka and Y. Shimakawa, *Jap. J. Appl. Phys.*, 2009, **48**, 010216
[40] M. H. K. Rubel, A. Miura, T. Takei, N. Kumada, M. M. Ali, M. Nagao, S. Watauchi, I. Tanaka, K. Oka, M. Azuma, E. Magome, C. Moriyoshi, Y. Kuroiwa and A. K. M. A. Islam, *Angew. Chem., Int. Ed.*, 2014, **53**, 3599-3603.
[41] M. H. K. Rubel, T. Takei, N. Kumada, M. M. Ali, A. Miura, K. Tadanaga, K. Oka, M. Azuma, E. Magomae, C. Moriyoshi and Y. Kuroiwa, *J. Alloys. Comp.*, 2015, **634**, 208-214.
[42] M. H. K. Rubel, T. Takei, N. Kumada, M. M. Ali, A. Miura, K. Tadanaga, K. Oka, M. Azuma, M. Yashima, K. Fujii, E. Magome, C. Moriyoshi, Y. Kuroiwa, J. R. Hester and M. Aydeev, *Chem. Mater.*, 2016, **28**, 459-465.

[43] A. W. Sleight, J. L. Gillson and P. E. Bierstedt, *Solid State Commun*, 1975, **17**, 27-28; R. J. Cava, B. Batlogg, J. J. Krajewski, R. Farrow, L. W. Rupp, A. E. White, K. Short, W. F. Peck and T. Kometani, *Nature*, 1988, **332**, 814-816.
[44] A. Trovarelli, *Catal. Rev.-Sci. Eng.*, 1996, **38**, 439-520; A. Trovarelli and P. Fornasiero, *Catalysis by Ceria and Related Materials, 2nd Edition* Imperial College Press, London, 2013.
[45] S. Hilaire, X. Wang, T. Luo, R. J. Gorte and J. Wagner, *Appl. Catal. A-Gen.*, 2001, **215**, 271-278.
[46] R. Di Monte and J. Kašpar, *Topics in Catalysis*, 2004, **28**, 47-57; R. J. Gorte, *AIChE Journal*, 2010, **56**, 1126-1135.
[47] M. Cargnello, J. J. D. Jaén, J. C. H. Garrido, K. Bakhmutsky, T. Montini, J. J. C. Gámez, R. J. Gorte and P. Fornasiero, *Science*, 2012, **337**, 713-717; S. Colussi, A. Gayen, M. F. Camellone, M. Boaro, J. Llorca, S. Fabris and A. Trovarelli, *Angew. Chem., Int. Ed.*, 2009, **48**, 8481-8484.
[48] W. C. Chueh, C. Falter, M. Abbott, D. Scipio, P. Furler, S. M. Haile and A. Steinfeld, *Science*, 2010, **330**, 1797-1801; C. L. Muhich, B. W. Evanko, K. C. Weston, P. Lichty, X. Liang, J. Martinek, C. B. Musgrave and A. W. Weimer, *Science*, 2013, **341**, 540-542.
[49] X. D. Feng, D. C. Sayle, Z. L. Wang, M. S. Paras, B. Santora, A. C. Sutorik, T. X. T. Sayle, Y. Yang, Y. Ding, X. D. Wang and Y. S. Her, *Science*, 2006, **312**, 1504-1508.
[50] S. Yabe and T. Sato, *J. Solid State Chem.*, 2003, **171**, 7-11.
[51] X. Q. Fu, C. Wang, H. C. Yu, Y. G. Wang and T. H. Wang, *Nanotechnology*, 2007, **18**, 145503.
[52] R. Di Monte and J. Kašpar, *J. Mater. Chem.*, 2005, **15**, 633-648.
[53] R. I. Walton, *Prog. Cryst. Growth Charact. Mater.*, 2011, **57**, 93-108.
[54] G. S. Li, R. L. Smith and H. Inomata, *J. Amer. Chem. Soc.*, 2001, **123**, 11091-11092.
[55] S. Hull, S. T. Norberg, M. G. Tucker, S. G. Eriksson, C. E. Mohn and S. Stolen, *Dalton Trans.*, 2009, 8737-8745.
[56] K. Sardar, H. Y. Playford, R. J. Darton, E. R. Barney, A. C. Hannon, D. Tompsett, J. Fisher, R. J. Kashtiban, J. Sloan, S. Ramos, G. Cibin and R. I. Walton, *Chem. Mater.*, 2010, **22**, 6191-6201.
[57] J. Beckers, A. F. Lee and G. Rothenberg, *Adv. Syn. Catal.*, 2009, **351**, 1557-1566.
[58] C. I. Hiley, J. M. Fisher, D. Thompsett, R. J. Kashtiban, J. Sloan and R. I. Walton, *J. Mater. Chem. A*, 2015, **3**, 13072-13079.
[59] K. Hashimoto, H. Irie and A. Fujishima, *Jap. J. Appl. Phys.*, 2005, **44**, 8269-8285; M. Ni, M. K. H. Leung, D. Y. C. Leung and K. Sumathy, *Renewable & Sustainable Energy Reviews*, 2007, **11**, 401-425; X. Chen and S. S. Mao, *Chem. Rev.*, 2007, **107**, 2891-2959; A. Fujishima, X. T. Zhang and D. A. Tryk, *Surf. Sci. Rep.*, 2008, **63**, 515-582.
[60] K. Tomita, V. Petrykin, M. Kobayashi, M. Shiro, M. Yoshimura and M. Kakihana, *Angew. Chem., Int. Ed.*, 2006, **45**, 2378-2381; T. A. Kandiel, R. Dillert, A. Feldhoff and D. W. Bahnemann, *J. Phys. Chem. C*, 2010, **114**, 4909-4915.
[61] Y. Ide, N. Inami, H. Hattori, K. Saito, M. Sohmiya, N. Tsunoji, K. Komaguchi, T. Sano, Y. Bando, D. Golberg and Y. Sugahara, *Angew. Chem., Int. Ed.*, 2016, **55**, 3600-3605.
[62] D. L. Burnett, M. H. Harunsani, R. J. Kashtiban, H. Y. Playford, J. Sloan, A. C. Hannon and R. I. Walton, *J. Solid State Chem.*, 2014, **214**, 30-37.
[63] M. Xu, P. M. Da, H. Y. Wu, D. Y. Zhao and G. F. Zheng, *Nano Letters*, 2012, **12**, 1503-1508.

[64] T. D. Nguyen-Phan, S. Luo, D. Vovchok, J. Llorca, S. Sallis, S. Kattel, W. Q. Xu, L. F. J. Piper, D. E. Polyansky, S. D. Senanayake, D. J. Stacchiola and J. A. Rodriguez, *Phys. Chem., Chem. Phys.*, 2016, **18**, 15972-15979.
[65] Q. J. Zhang, Y. Fu, Y. F. Wu and T. Y. Zuo, *Eur. J. Inorg. Chem.*, 2016, 1706-1711.
[66] J. F. de Lima, M. H. Harunsani, D. J. Martin, D. Kong, P. W. Dunne, D. Gianolio, R. J. Kashtiban, J. Sloan, O. A. Serra, J. W. Tang and R. I. Walton, *J. Mater. Chem. A*, 2015, **3**, 9890-9898.
[67] Z. L. He, W. X. Que, J. Chen, X. T. Yin, Y. C. He and J. B. Ren, *ACS Appl. Mater. Inter.*, 2012, **4**, 6815-6825; J. Li, M. Yang and Z. B. Jiang, *Chin. Chem. Lett.*, 2014, **25**, 283-286.
[68] B. Liu, L. M. Liu, X. F. Lang, H. Y. Wang, X. W. Lou and E. S. Aydil, *Ener. Environ. Sci.*, 2014, **7**, 2592-2597.
[69] K. Chen and D. Xue, *CrystEngComm*, 2012, **14**, 8068-8075.
[70] K. Chen, C. Sun and D. Xue, *Phys. Chem., Chem. Phys.*, 2015, **17**, 732-750.
[71] Y. Xu, H. Hao, P. Liu, Q. Wang, Y. Sun and G. Zhang, *CrystEngComm*, 2014, **16**, 10451-10459.
[72] J. Yin, F. Gao, C. Wei and Q. Lu, *Sci. Rep.*, 2014, **4**.
[73] S. Das, K. Dutta and A. Pramanik, *CrystEngComm*, 2013, **15**, 6349-6358.
[74] X. J. Wang, Q. L. Zhang, Q. A. Wan, G. Z. Dai, C. J. Zhou and B. S. Zou, *J. Phys. Chem. C*, 2011, **115**, 2769-2775.
[75] M. Raula, M. H. Rashid, T. K. Paira, E. Dinda and T. K. Mandal, *Langmuir*, 2010, **26**, 8769-8782.
[76] A. Lamberti, N. Garino, K. Bejtka, S. Bianco, S. Stassi, A. Chiodoni, G. Canavese, C. F. Pirri and M. Quaglio, *New. J. Chem,*, 2014, **38**, 2024-2030.
[77] D. Caruntu, T. Rostamzadeh, T. Costanzo, S. S. Parizi and G. Caruntu, *Nanoscale*, 2015, **7**, 12955-12969.
[78] C. Friderichs, N. Zotov and W. Mader, *Eur. J. Inorg. Chem.*, 2015, 288-295.
[79] J. Spooren, A. Rumplecker, F. Millange and R. I. Walton, *Chem. Mater.*, 2003, **15**, 1401-1403.
[80] J. Spooren and R. I. Walton, *J. Solid State Chem.*, 2005, **178**, 1683-1691.
[81] M. H. Harunsani, J. Li, Y. B. Qin, H. T. Tian, J. Q. Li, H. X. Yang and R. I. Walton, *Appl. Phys. Lett.*, 2015, **107**.
[82] I. N. Gonzalez-Jimenez, A. Torres-Pardo, M. Garcia-Hernandez, J. M. Gonzalez-Calbet, M. Parras and A. Varela, *Crys. Growth Des.*, 2015, **15**, 2192-2203.
[83] D. Makovec, T. Gorsak, K. Zupan and D. Lisjak, *J. Cryst. Growth*, 2013, **375**, 78-83.
[84] K. Huang, W. Feng, L. Yuan, J. Zhang, X. Chu, C. Hou, X. Wu and S. Feng, *CrystEngComm*, 2014, **16**, 9842-9846.
[85] S. Yin, H. Tian, Z. Ren, X. Wei, C. Chao, J. Pei, X. Li, G. Xu, G. Shen and G. Han, *Chem. Commun.*, 2014, **50**, 6027-6030.
[86] K. M. Ø. Jensen, C. Tyrsted, M. Bremholm and B. B. Iversen, *ChemSusChem*, 2014, **7**, 1594-1611.
[87] C. Tyrsted, K. M. Ø. Jensen, E. D. Bojesen, N. Lock, M. Christensen, S. J. L. Billinge and B. B. Iversen, *Angew. Chem., Int. Ed.*, 2012, **51**, 9030-9033.
[88] K. M. Ø. Jensen, M. Christensen, P. Juhas, C. Tyrsted, E. D. Bojesen, N. Lock, S. J. L. Billinge and B. B. Iversen, *J. Amer. Chem. Soc.*, 2012, **134**, 6785-6792.
[89] D. Saha, K. M. Ø. Jensen, C. Tyrsted, E. D. Bojesen, A. H. Mamakhel, A. C. Dippel, M. Christensen and B. B. Iversen, *Angew. Chem., Int. Ed.*, 2014, **53**, 3667-3670.
[90] F. Xia, D. H. Chen, N. V. Y. Scarlett, I. C. Madsen, D. Lau, M. Leoni, J. Ilavsky, H. E. A. Brand and R. A. Caruso, *Chem. Mater.*, 2014, **26**, 4563-4571.

[91] S. M. Woodley and R. Catlow, *Nat. Mater.*, 2008, **7**, 937-946; S. Curtarolo, G. L. W. Hart, M. B. Nardelli, N. Mingo, S. Sanvito and O. Levy, *Nat. Mater.*, 2013, **12**, 191-201; S. V. Kalinin, B. G. Sumpter and R. K. Archibald, *Nat. Mater.*, 2015, **14**, 973-980.
[92] P. Raccuglia, K. C. Elbert, P. D. F. Adler, C. Falk, M. B. Wenny, A. Mollo, M. Zeller, S. A. Friedler, J. Schrier and A. J. Norquist, *Nature*, 2016, **533**, 73-76.
[93] M. M. Lencka and R. E. Riman, *Chem. Mater.*, 1993, **5**, 61-70.
[94] P. W. Dunne, A. S. Munn, C. L. Starkey, T. A. Huddle and E. H. Lester, *Phil. Trans. Royal. Soc. A*, 2015, **373**, 20150015.

Figure Captions

Figure 1: Structures of alkali-earth iridium hydroxides and oxides crystallised by using hydrothermal chemistry.[26]

Figure 2: A phase diagram representation of composition space for the synthesis of alkali-earth ruthenates and oxyhydroxides. Red circles represent hydrothermally prepared materials with closed circles those materials prepared in our work at 200 °C, [27-29]open red circles the work of others and black circles are those materials prepared using solid-state synthesis. Coloured zones indicate ruthenium average oxidation state of < 4 (green), between 4 and 5 (blue) and > 5 (pink), with boundaries as dotted lines. A full list of compositions and literature references is available in the ESI.

Figure 3: Representation of the pyrochlore structure with (a) showing a single unit cell with cyan eight-coordinate A-centred polyhedra and green six-coordinated B-centred polyhedra and (b) showing the connectivity of A- and B-centred polyhedra for the case where the B-site is a regular octahedron. The table gives a summary of A and B combinations found in ruthenate and iridates prepared using hydrothermal methods.

Figure 4: Structures of perovskites found for novel bismuthates produced from hydrothermal chemistry:[39-42] (a) shows the conventional perovskite ABO_3, as found for $(Ba_{0.82}K_{0.18})(Bi_{0.53}Pb_{0.47})O_3$ where the A-site and B-site substituents are randomly distributed and (b) shows the A-site ordered $A'A''_3B_4O_{12}$ structure found for $(Ba_{0:75}K_{0:14}H_{0:11})BiO_3 \cdot nH_2O$, $(Na_{0.25}K_{0.45})Ba_3Bi_4O_{12}$, and $KBa_3(Bi_{0.89}Na_{0.11})_4O_{12}$, where A-site metals show long range order (represented by the orange and blue spheres). The purple octahedral represent the B site in both cases.

Figure 5: A Periodic Table of substituted ceria, $Ce_{1-x}M_xO_{2-y}$ or $CeO_{2-z}E_z$. The shades of blue represent different levels of substitution that have been reported in the literature, with the green borders highlighting materials produced by hydrothermal reactions. Also shaded are the cases of anion-substituted materials (in yellow). Further details and literature references are provided in the ESI.

Figure 6: Pd-substituted ceria from hydrothermal synthesis. The left images are elemental maps measured using electron microscopy that show the distribution of Ce and Pd, while the EXAFS spectrum measured at the Pd L_{III}-edge (bottom right) can be fitted to a model with Ce^{4+} replaced by Pd^{2+} and the substituent located in interstitial square-planar sites as indicated on the top right. Reproduced from Ref. [58] with permission from the Royal Society of Chemistry.

Figure 7: Crystal structure models for pure anatase (a) and carbonate substituted TiO_2 (b). The lower panels show two different calculations of band structure for the two situations showing the reduction in band gap for the substituted material. Reproduced from Ref. [68] with permission from the Royal Society of Chemistry.

Figure 8: SEM images of different Cu_2O morphologies obtained with different concentrations of NaOH in the work of Chen and Xue. Scale bars: (a, b) 500 nm, (c–o) 1 μm, insets in (d–o) 200 nm. Reproduced from Ref. [69] with permission from the Royal Society of Chemistry.

Figure 9: Facetted Fe_3O_4 polyhedral crystals produced from solvothermal synthesis in a mixed solvent of ethylene glycol and H_2O. Facet assignments are shown from simulation in panel a, while individual polyhedral nanoparticles viewed from different directions are shown in b–e. Scale bar = 200 nm. Reproduced from Ref. [71] with permission from the Royal Society of Chemistry.

Figure 10: Morphologies of ZnO reported by Yin *et al.* from solvothermal synthesis in mixed water-ethanol solvent in the presence of gylcine.[72] Panels a – j denote increasing quantities of water used in the synthesis from. Reprinted by permission from Macmillan Publishers Ltd: *Scientific Reports* 4, 3736, copyright (2014).

Figure 11: TEM images of nanotube arrays of (a) TiO_2 and (b-e) $BaTiO_3$ produced after hydrothermal treatment (150 °C for 2 h with a 0.1 M barium acetate) with varying concentrations of KOH (0.05, 0.1, 0.25 and 1 M, respectively). (f) shows a bright field TEM image of the sample in (d). Reproduced from Ref. [76] with permission from the

Centre National de la Recherche Scientifique (CNRS) and the Royal Society of Chemistry.

Figure 12: TEM micrographs of variable-size $BaTiO_3$ cuboidal nanocrystals obtained by varying the concentration of the precursors in solvothermal reactions. Reproduced from Ref. [77] with permission from the Royal Society of Chemistry.

Figure 13: $La_{0.75}Sr_{0.25}MnO_3$ microstructures crystallised in a 260 °C hydrothermal environment in the presence of ammonium ions. Reproduced from Ref. [84] with permission from the Royal Society of Chemistry.

Table of Contents Entry

Three aspects in the synthesis of oxides under solvothermal conditions are reviewed: materials discovery, substitutional chemistry and crystal habit control.

Biographies

Craig Hiley received his MChem degree in Chemistry from the University of Warwick in 2010, where he remained to complete a PhD under the supervision of Professor Richard Walton titled *New Oxides for Catalysis from Hydrothermal Synthesis* (2014). He is currently a postdoctoral research associate at the University of Liverpool in the group of Professor Matthew Rosseinsky FRS.

Richard Walton is Professor of Inorganic Chemistry at the University of Warwick and his research focuses on developing novel synthesis methods for solid-state materials and structural characterisation to develop structure-property relationships. He is also presently Royal Society Industry Fellow, working with Johnson Matthey plc to examine the applications of new materials in various technologies. His research regularly makes use of synchrotron X-ray and central neutron facilities for materials characterisation, with particular emphasis on *in situ* methods for following crystallisation. He is an editor of the *Inorganic Materials* book series, with Bruce and O'Hare.

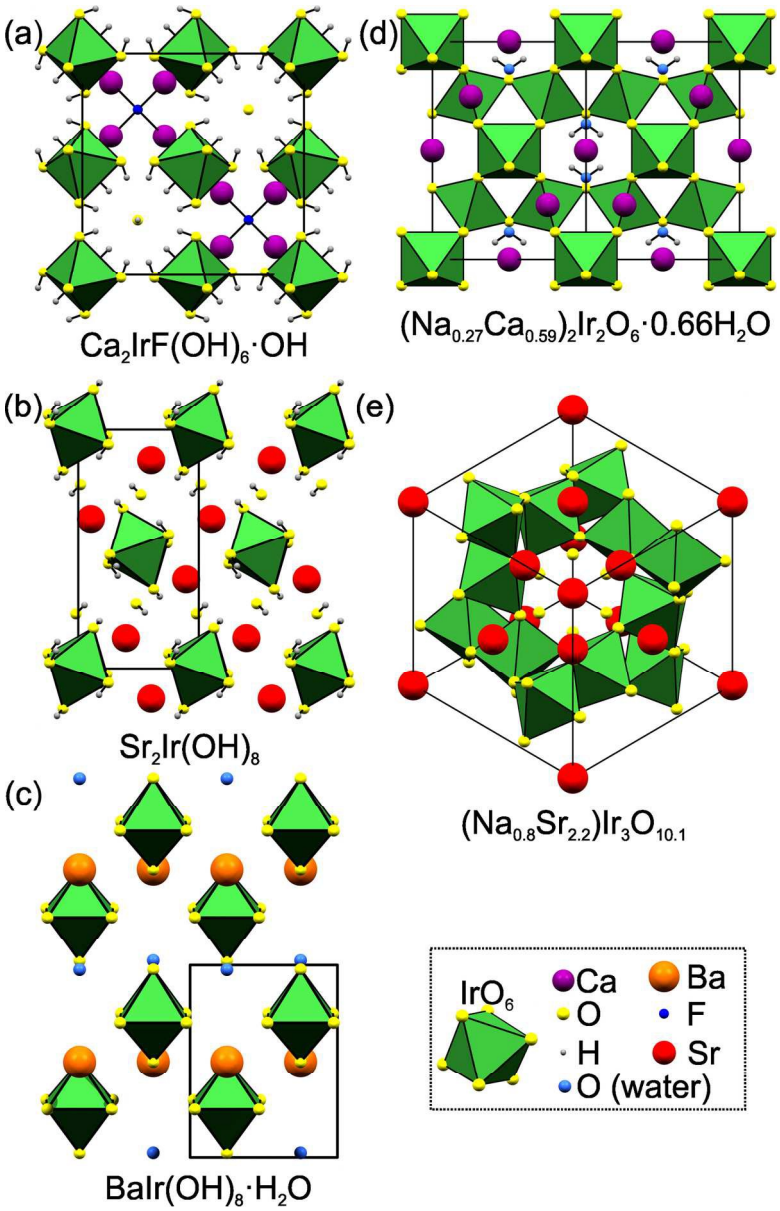

130x203mm (300 x 300 DPI)

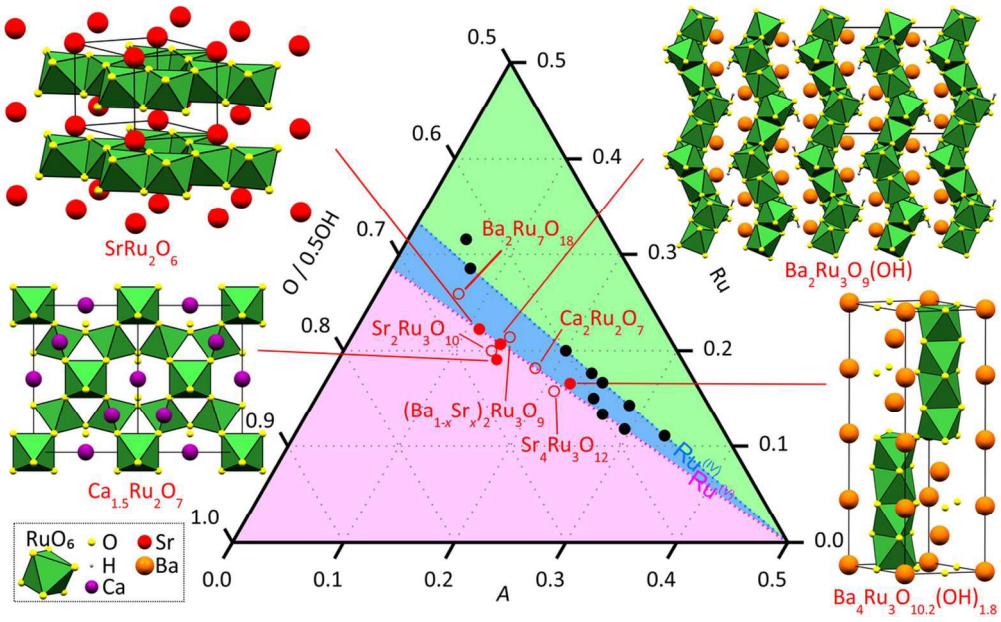

110x67mm (300 x 300 DPI)

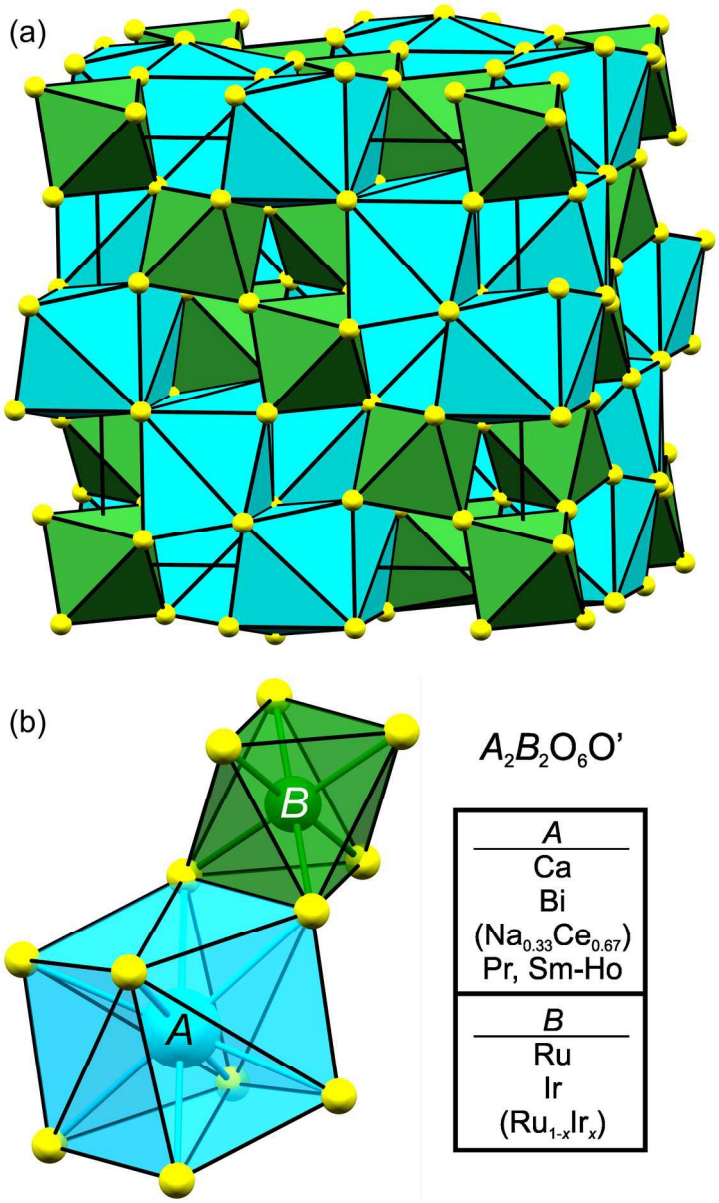

139x233mm (300 x 300 DPI)

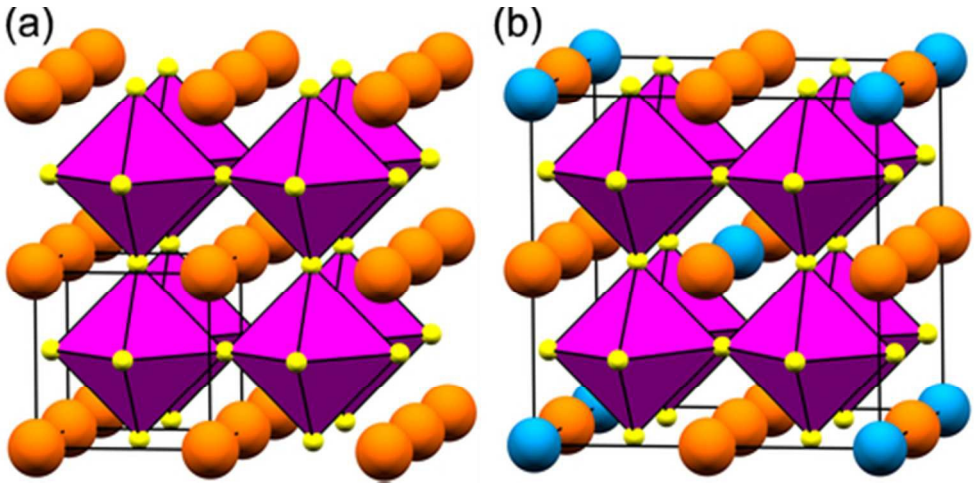

41x20mm (300 x 300 DPI)

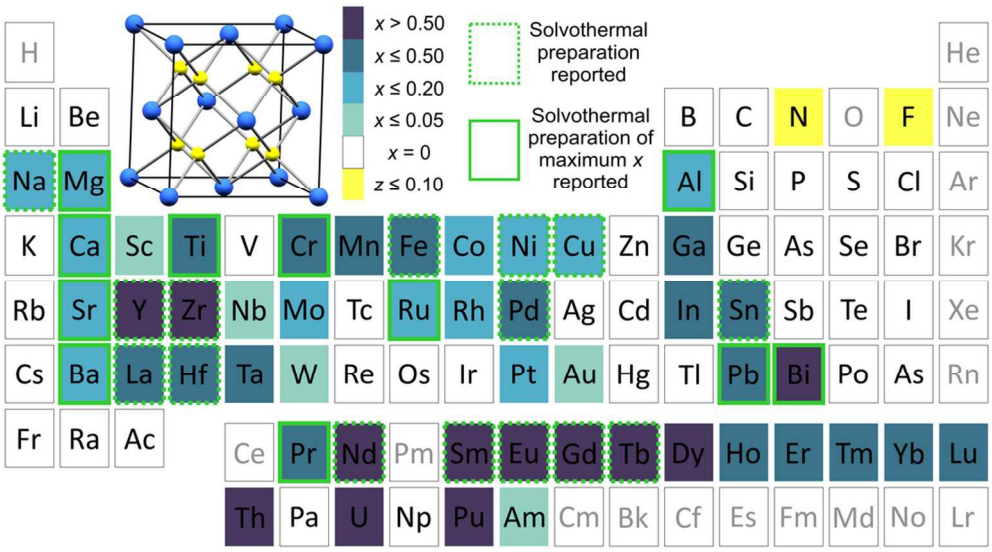

99x55mm (300 x 300 DPI)

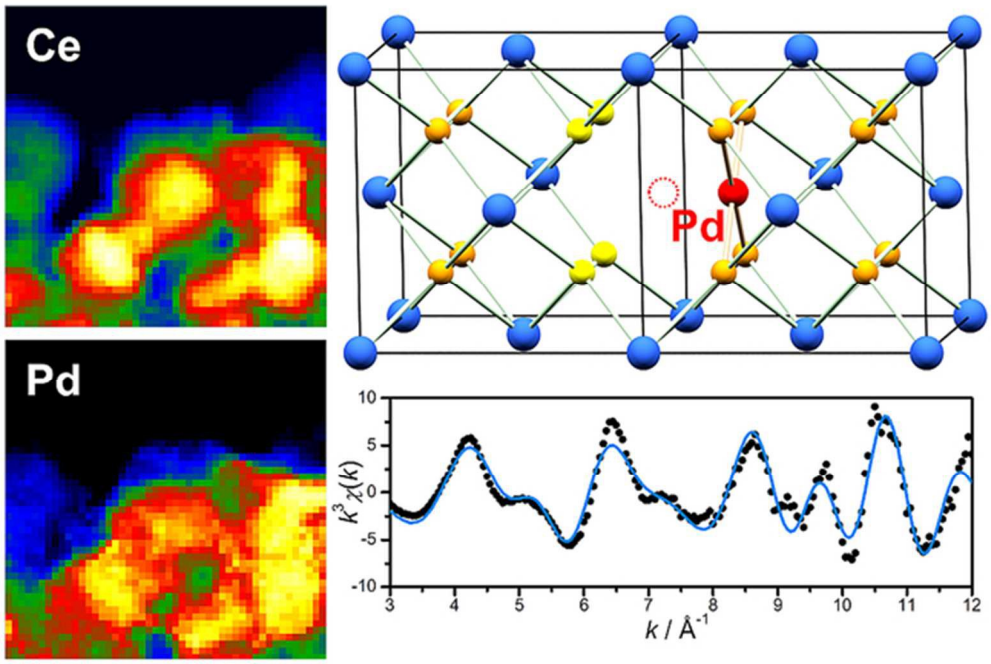

55x36mm (300 x 300 DPI)

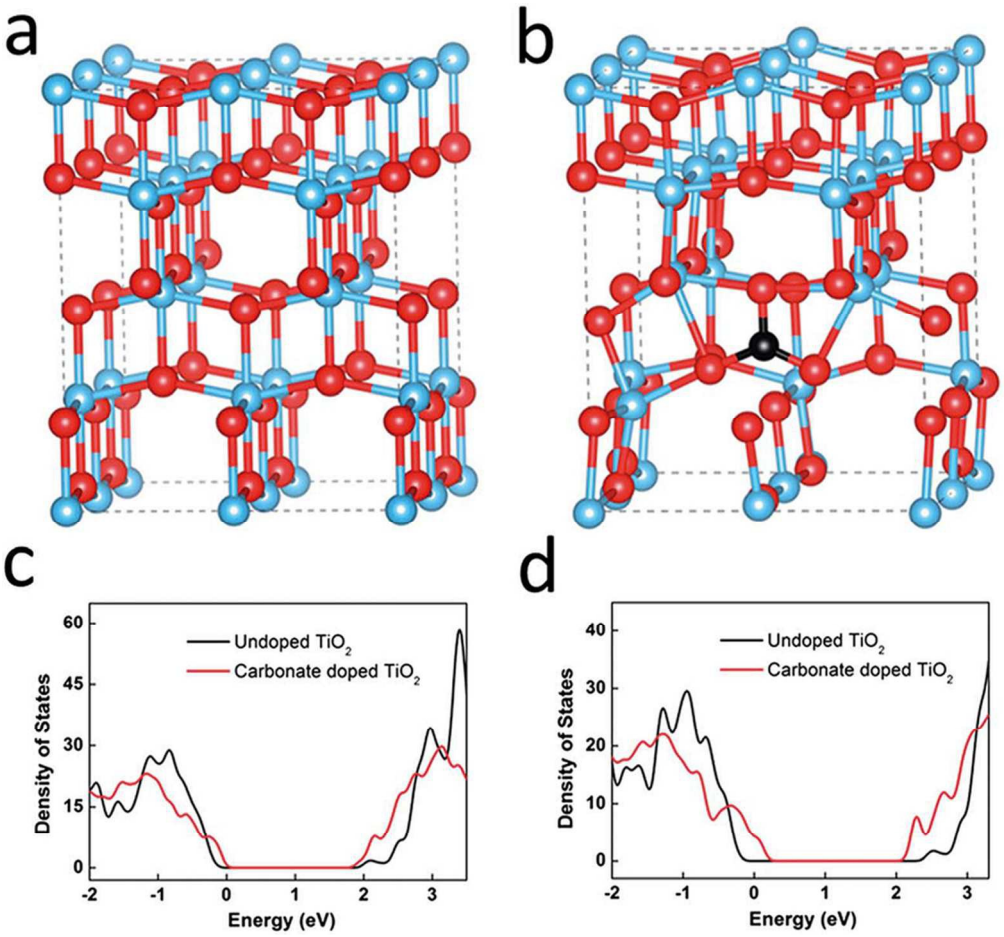

77x71mm (300 x 300 DPI)

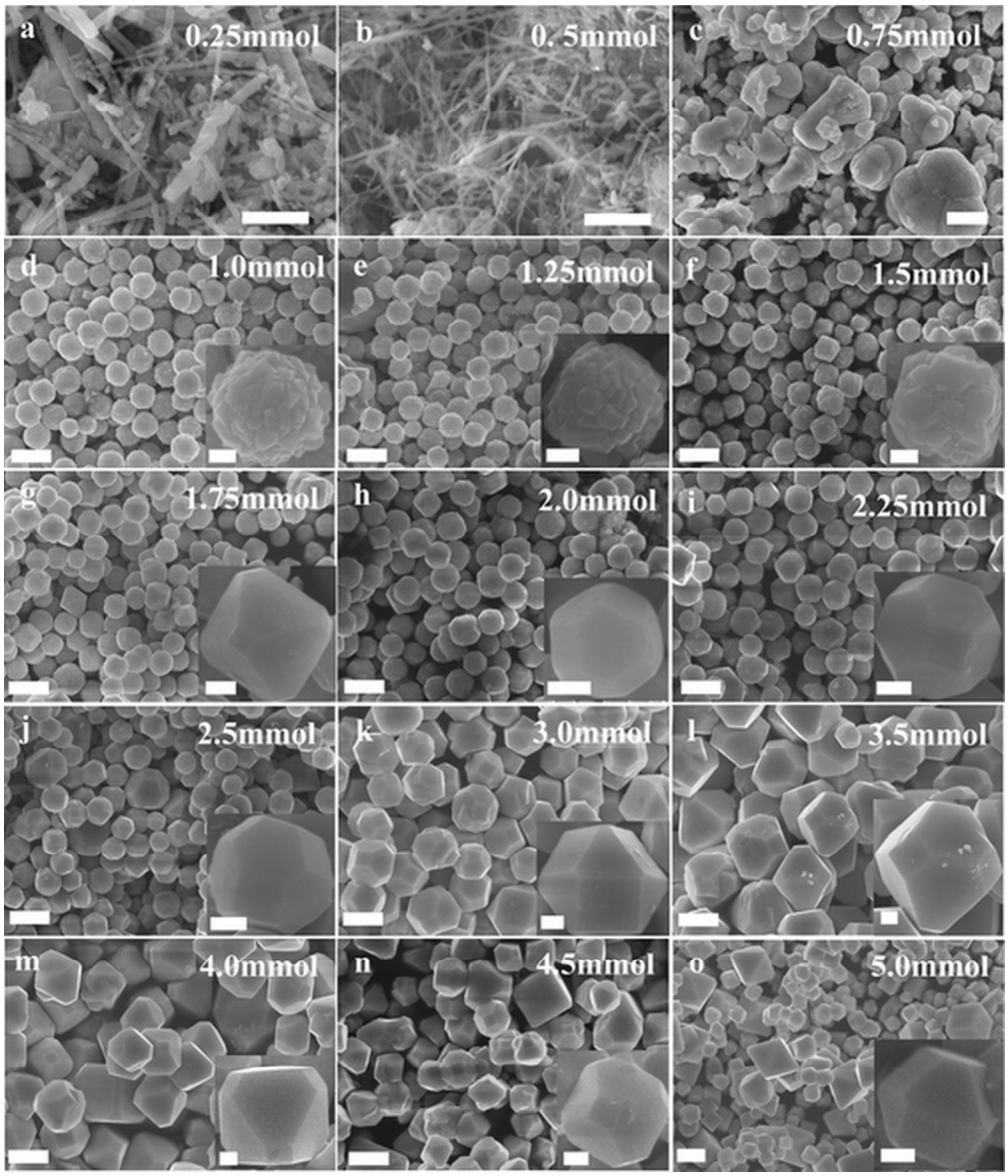

96x113mm (300 x 300 DPI)

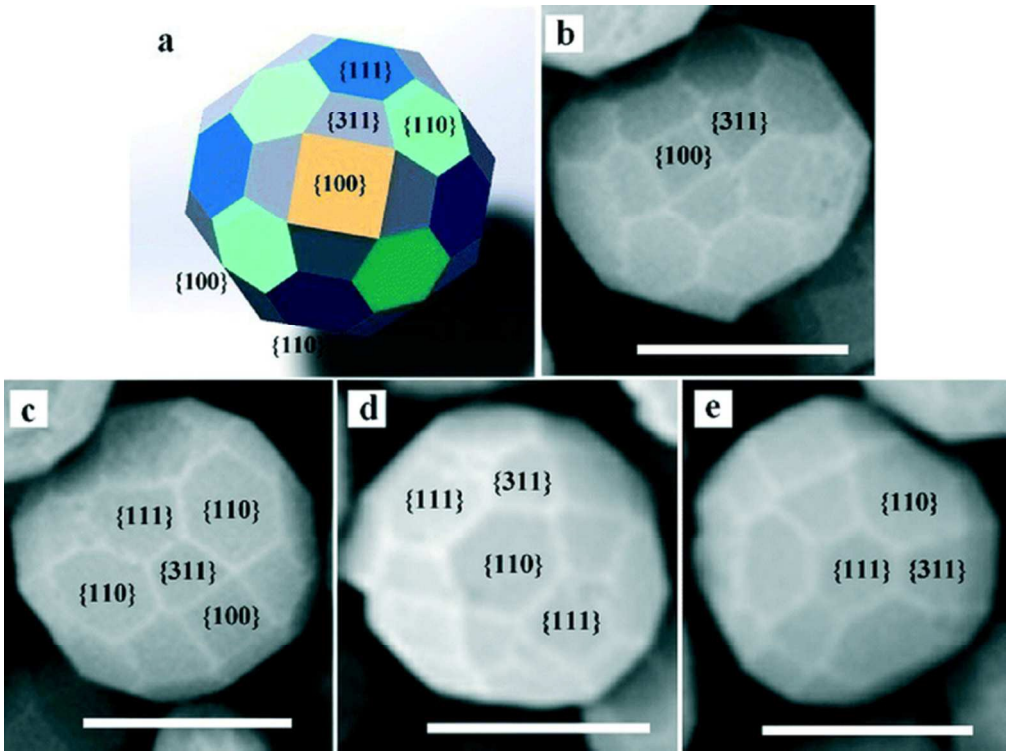

61x46mm (300 x 300 DPI)

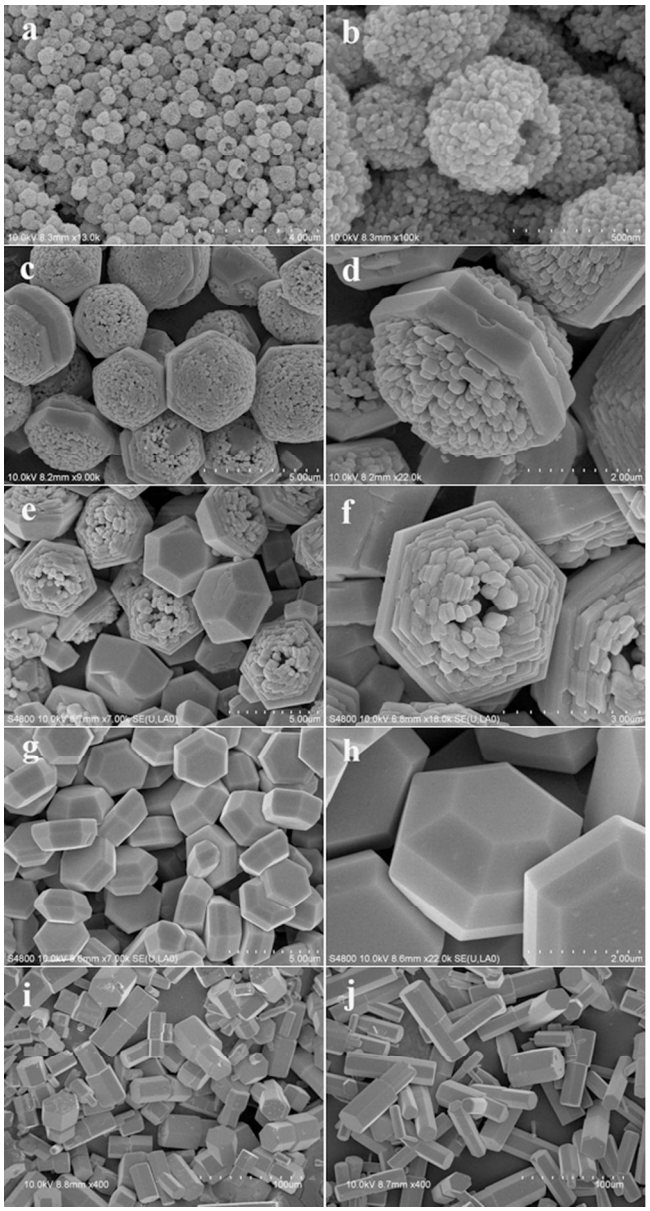

155x291mm (300 x 300 DPI)

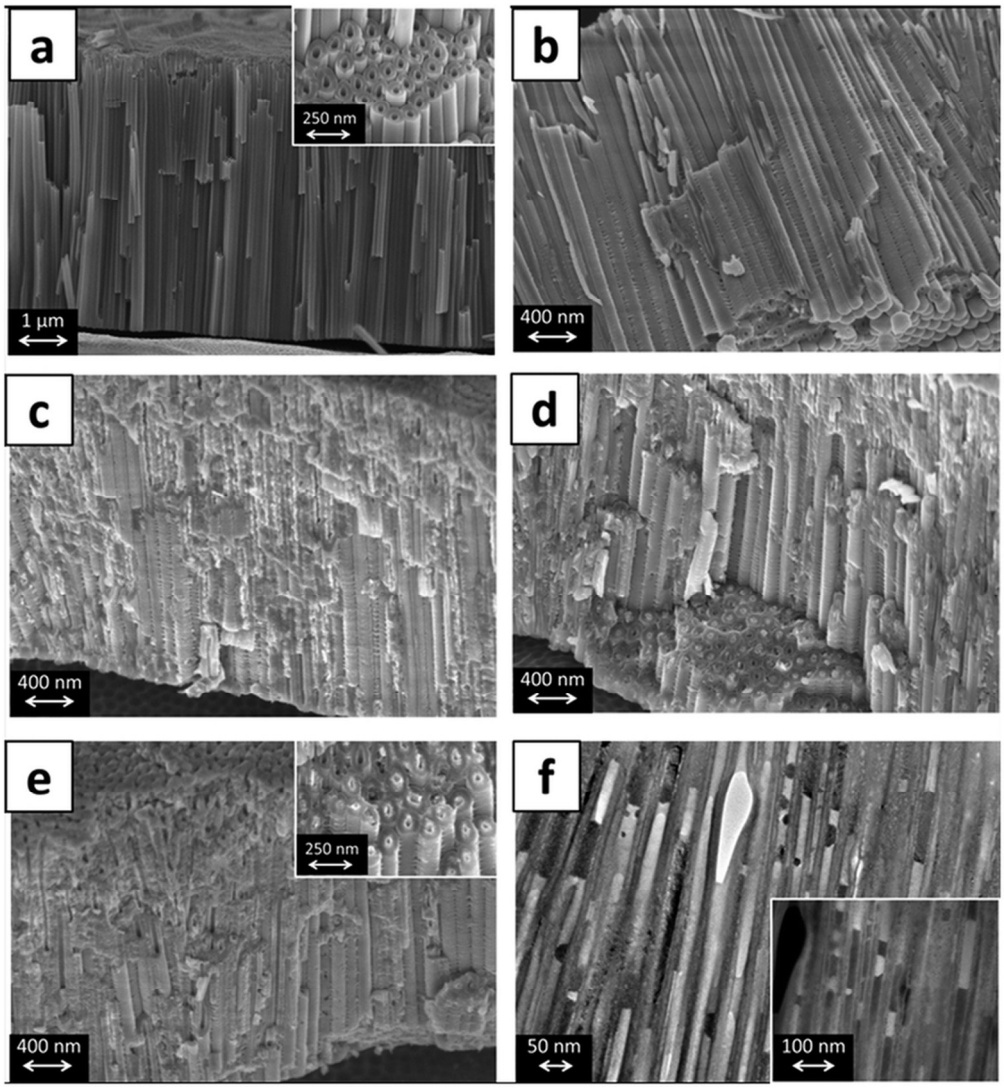

89x97mm (300 x 300 DPI)

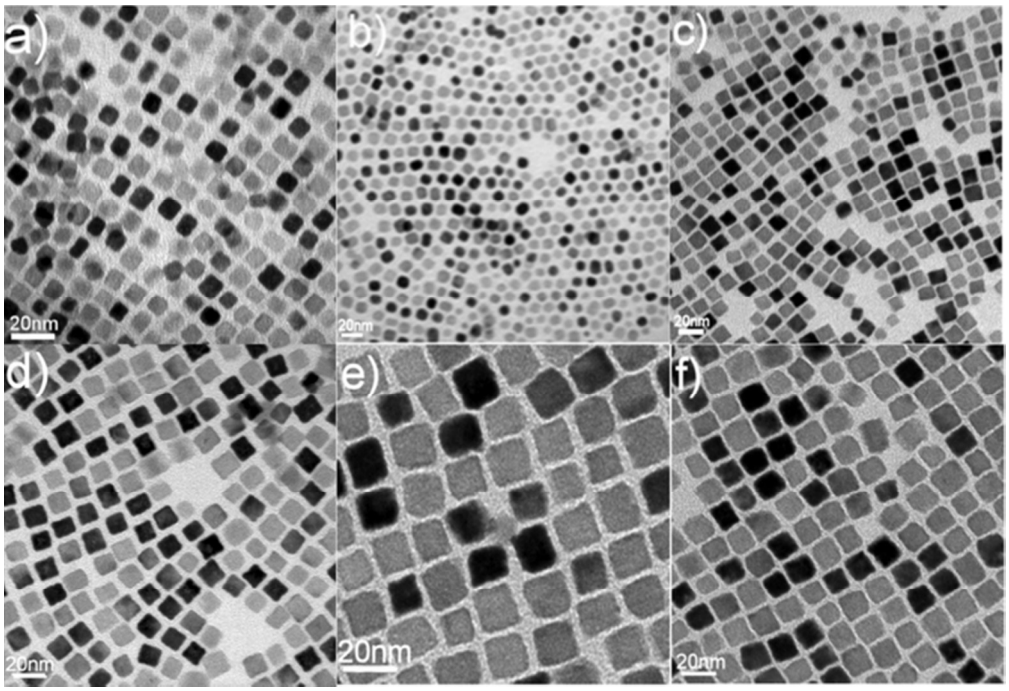

56x38mm (300 x 300 DPI)

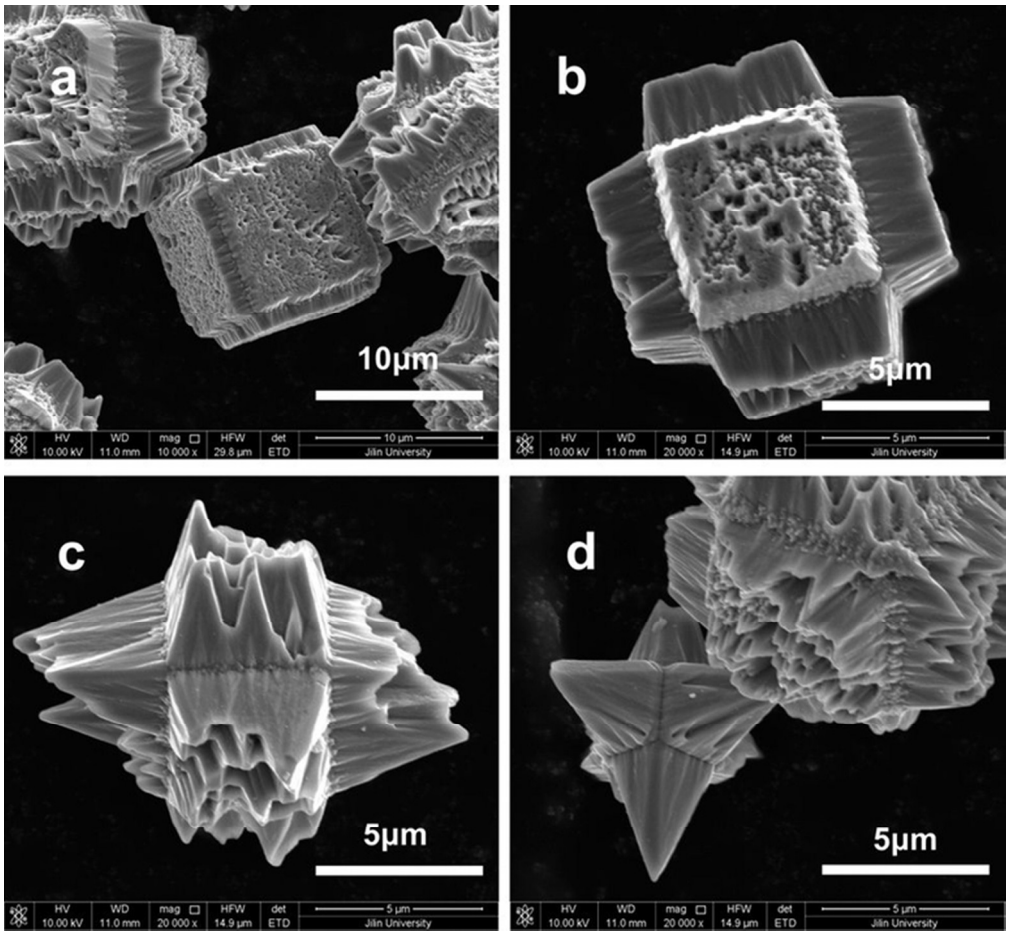

65x60mm (300 x 300 DPI)